MATHEMATICAL BIOSCIENCES
AND ENGINEERING
Volume **3**, Number **4**, September **2006**

http://www.mbejournal.org/

pp. **615–634**

MATHEMATICAL MODELING OF BIOWALL REACTORS FOR IN-SITU GROUNDWATER TREATMENT

Donna J. Cedio-Fengya

Department of Mathematics
William Paterson University, Wayne, NJ 07470

John G. Stevens

Department of Mathematical Sciences
Montclair State University, Montclair N.J. 07043

(Communicated by Erik Bollt)

Abstract. In this paper we develop a comprehensive model for the remediation of contaminated groundwater in a passive, in-ground reactor, generally known as a biowall. The model is based on our understanding of the component transport and biokinetic processes that occur as water passes through a bed of inert particles on which a biofilm containing active microbial degraders, typically aerobic bacteria, is developing. We give a detailed derivation of the model based on accepted engineering formulations that account for the mass transport of the contaminant (substrate) to the surface of the biofilm, its diffusion into the biofilm to the proximity of a microbe, and its subsequent destruction within that degrader. The model has been solved numerically and incorporated in a robust computer code. Based on representative input values, the results of varying key parameters in the model are presented. The relation between biofilm growth and biowall performance is explored, revealing that the amount of biomass and its distribution within the biowall are key parameters affecting contaminant removal.

1. **Introduction.** Much of the U.S. population relies on groundwater for its potable water, but some groundwater aquifers have been contaminated with hazardous organic chemicals. Numerous pesticides, wood preservatives and other aromatic and chlorinated hydrocarbons have been identified as priority substances contaminating groundwater. Representative contaminants include benzene, methyl-tert-butyl-ether (MTBE) and trichloroethylene (TCE). These chemicals are often by-products of agricultural and industrial production or come from leaks from storage tanks. Efficient management and clean-up of contaminated groundwater plumes is a challenging environmental problem. Pump-and-treat technology, in which groundwater is pumped to the surface and treated in surface facilities, has been available for many years. However it is now recognized throughout the remediation community that pump-and-treat systems cannot restore groundwater quality and meet clean-up objectives, or can do so only at an exorbitant cost. As a result there is growing need for developing simple, inexpensive treatment technologies to clean up contaminated groundwater.

2000 *Mathematics Subject Classification.* 35K57, 65M99, and 92B99.

Key words and phrases. aerobic degradation, biofilm, biowall, heterotophic metabolism, in-situ bioremediation.

Recent research in groundwater remediation has focused on the ability of bacteria to degrade various man-made chemicals. Biological technology presents a cost-effective and environmentally friendly alternative to conventional pump-and-treat technology for remediating contaminated groundwater. Air emissions and excavation costs are minimized by treating groundwater in situ. One novel in-situ treatment that has received a considerable amount of attention is the construction of a biowall, as illustrated in Figure 1 below. A biowall is an activated area constructed downstream of a contaminated groundwater plume. Often cutoff walls are installed to direct or funnel the flow of groundwater into the biowall. The biowall is initially packed with an inert material (e.g., gravel) on which the biofilm will develop. In the biowall, bacteria, typically already present in the groundwater, are stimulated, usually by aeration, nutrient addition,or both, to form the biofilm on the bed material. Within the biofilm are active aerobic microbes (such as "pseudomonas" [4], [11]) that, in the presence of dissolved oxygen, degrade the pollutants passing through the groundwater to less toxic or nontoxic forms. Before water enters the biowall this reaction is limited by lack of oxygen, which is virtually depleted in the groundwater. Biowalls are typically aerated so that the oxygen limitation is removed. Although anaerobic degradation also occurs, it is typically much slower than aerobic degradation. These in-ground bioreactors provide a flexible and economical means to controlling contaminant plumes and can also be used in combination with conventional pump and treat techniques.

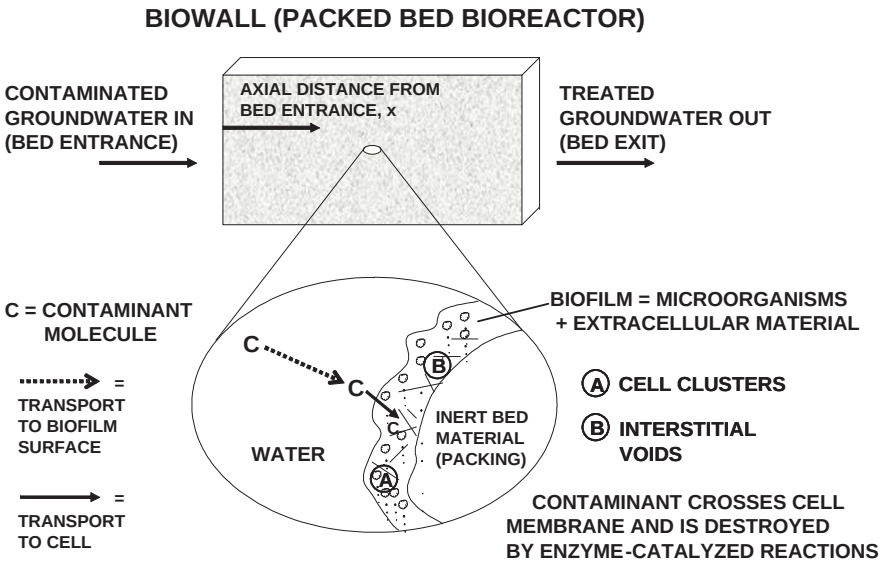

FIGURE 1. Schematics of a biowall exhibiting its component processes.

2. **Biofilm reactor systems.** Many investigators have studied the degradation of organic compounds in biofilm systems. Laser confocal microscopy has been used to examine the structure of the biofilm as it develops. Microelectrode techniques have

been employed to evaluate the chemical kinetics occurring within the biofilm. Most of these studies have been carried out in batch or semi-batch reactors; fewer have been performed using flow reactors. Arcangeli and Arvin studied the degradation of toluene in a biofilm under both aerobic and anoxic conditions [1]. They used a continuously fed biodrum system that consisted of a cylinder rotating inside a stationary drum with the biofilm growing on both. A biochemical model for this system was developed that included the growth dynamics of the biofilm using the BIOSIM computer code, a predecessor of the AQUASIM program discussed below. Horn and Hempel investigated substrate utilization and mass transfer in a tubular flow reactor in which the biofilm developed on the surface of a glass tube [8]. They performed careful measurements of mean biofilm thickness and oxygen profiles and also simulated their results using AQUASIM. As we have indicated, AQUASIM is a frequently used tool for the identification and simulation of aquatic systems [10]. Indeed, more than 130 publications reporting applications of this software are given at http://www.aquasim.eawag.ch/e_aquasim_refs.html. Of these, few fall into the category of advective-diffusive biofilm reactor systems. AQUASIM facilitates the formulation and solution of a wide variety of mathematical models describing environmental systems. The user chooses model variables and selects from a variety of reactor compartments that are then appropriately linked to complete the model specification. Because of novel features of the biowall model that we derive (e.g., accounting for the change in local bed porosity that results from biofilm growth), it is not clear that we could have efficiently implemented it using AQUASIM. Rather, we have chosen a numerical technique that we have used successfully in several applications.

3. **The biowall model.** In this paper we develop a comprehensive computational biowall performance model that can be used as both a design and an optimization tool. Our model is based on our understanding of the component transport and biokinetic processes as water passes over the gravel on which a biofilm is developing. We are primarily concerned with the biodegradation of the target contaminant by microbes present in the biofilm that has developed on the surface of the bed material. The key component processes in this degradation are the mass transport of the contaminant to the surface of the biofilm, its diffusion into the biofilm to the proximity of an active microbial degrader cell, and its subsequent diffusion into and reaction within that cell. We develop submodels for each of these component processes. We combine the individual submodels into an overall system model and investigate their complex interactions on the performance of the treatment cell.

Understanding biowall reactor performance presents several challenges. The approach and level of detail used in our model development must be consistent with our model objectives. Because it is important to understand the relation of biofilm growth and biowall performance, our model allows for the effect of biofilm thickness on the rate of contaminant degradation. To incorporate biofilm growth and inlet conditions that change in time, our model is a transient one. For the systems we will be studying, biofilm growth is quite slow due to the limited availability of carbon sources. As a consequence, there are two time scales in the problem, one for biodegradation of the contaminant and a much longer one for biofilm growth. We assume our system is oxygen rich so that oxygen concentration is not a rate-limiting factor. We can assume that degradation within the biofilm proceeds at the steady-state rate that would prevail for the current thickness. As a result, we

employ well-developed concepts used to describe mass transfer and reactions in packed beds to obtain an overall effective first-order degradation rate.

4. **Derivation of the governing equations.** In this section we derive a mathematical model for the biowall described above. Here we assume that the contaminant under consideration is the primary substrate (carbon source) for the microbes responsible for the biofilm growth, as would be the case in the event of the release of a single organic pollutant into clean groundwater. At the end of this section we discuss the generalization of this approach to the case of multiple substrates. Other assumptions on which our mathematical model will be developed are as follow:

i.) The flow field can be adequately described as axially dispersed plug flow.

ii). Mass transport of the substrate from the bulk flow to the biofilm surface can be modeled by the use of a mass-transfer coefficient.

iii.) An effectiveness factor can be used to obtain an effective first-order rate constant that includes the rates of diffusion and reaction within the biofilm.

iv.) A yield coefficient relates the utilization of the substrate to the growth of the biofilm.

v.) Biofilm growth changes the local porosity within the bed.

In addition to being defined when introduced, the symbols used, together with the description of the quantities they represent and their SI units, are compiled in the nomenclature found in Appendix A. Those variables that depend on axial location, x, and time, t, are indicated upon introduction and in Appendix A by the usual functional notation.

We first derive the substrate transport equation. We consider a control volume from x to $x + \Delta x$, where x is the axial distance from the entrance of the biowall. For the substrate,

$$\begin{aligned}
\text{Rate In} &= \text{Bulk Flow + Dispersion} \\
&= [\Omega U_i C](x,t) - D_{ax}\left[\Omega\Big(\frac{\partial}{\partial x}C\Big)\right](x,t),
\end{aligned}$$

$$\begin{aligned}
\text{Rate Out} &= \text{Bulk Flow + Dispersion + Mass Transfer to Biofilm Surface} \\
&= [\Omega U_i C](x+\Delta x,t) - D_{ax}\left[\Omega\Big(\frac{\partial}{\partial x}C\Big)\right](x+\Delta x,t) \\
&\qquad + A_r \int_x^{x+\Delta x} k_c a(\xi,t)(C(\xi,t) - C_s(\xi,t))d\xi,
\end{aligned}$$

and

$$\text{Rate of Accumulation} = \frac{\partial}{\partial t}\int_x^{x+\Delta x} [\Omega C](\xi,t)d\xi,$$

where $\Omega(x,t)$ is the open area of the bed cross-section, A_r is the total area of the bed cross-section, $a(x,t)$ is the area for mass transfer per bed volume, $U_i(x,t)$ is the interstitial velocity, D_{ax} is the axial dispersion coefficient, $C(x,t)$ is the

concentration of target pollutant, $C_s(x,t)$ is the concentration at the surface of biofilm, and k_c is the mass transfer coefficient.

Denoting the superficial velocity by U we note that ΩU_i equals $A_r U$ and remains constant. Therefore, applying the balance,

$$\text{Rate of Accumulation} = \text{Rate In - Rate Out}$$

yields

$$\begin{aligned}\frac{\partial}{\partial t}\int_x^{x+\Delta x}[\Omega C](\xi,t)d\xi \;&= A_r U\{C(x,t)-C(x+\Delta x,t)\}\\ &\quad + D_{ax}\left\{-\left[\Omega\big(\frac{\partial}{\partial x}C\big)\right](x,t)+\left[\Omega\big(\frac{\partial}{\partial x}C\big)\right](x+\Delta x,t)\right\}\\ &\quad - k_c A_r\int_x^{x+\Delta x} a(\xi,t)(C(\xi,t)-C_s(\xi,t))d\xi.\end{aligned}$$

Dividing by $A_r\Delta x$ and using the fact that the bed porosity $\varepsilon_b(x,t)=\frac{\Omega(x,t)}{A_r}$, we obtain

$$\begin{aligned}\frac{\frac{\partial}{\partial t}\int_x^{x+\Delta x}[\varepsilon_b C](\xi,t)d\xi}{\Delta x} \;&= U\left\{-\frac{C(x+\Delta x,t)-C(x,t)}{\Delta x}\right\}\\ &\quad + \frac{D_{ax}\left\{-\left[\varepsilon_b\big(\frac{\partial}{\partial x}C\big)\right](x,t)+\left[\varepsilon_b\big(\frac{\partial}{\partial x}C\big)\right](x+\Delta x,t)\right\}}{\Delta x}\\ &\quad - \frac{k_c\int_x^{x+\Delta x} a(\xi,t)(C(\xi,t)-C_s(\xi,t))d\xi}{\Delta x}.\end{aligned}$$

Letting $\Delta x\to 0$ gives the transport equation

$$\begin{aligned}\frac{\partial}{\partial t}[\varepsilon_b(x,t)C(x,t)] &= -U\left(\frac{\partial}{\partial x}C\right)(x,t)+D_{ax}\left(\frac{\partial}{\partial x}\left[\varepsilon_b\big(\frac{\partial}{\partial x}C\big)\right](x,t)\right)\\ &\quad - k_c a(x,t)(C(x,t)-C_s(x,t))\\ &= -U\left(\frac{\partial}{\partial x}C\right)(x,t)+D_{ax}\left(\frac{\partial}{\partial x}\left[\varepsilon_b\big(\frac{\partial}{\partial x}C\big)\right](x,t)\right)\\ &\quad - \kappa(x,t)C(x,t).\end{aligned}\tag{1}$$

where $k_c a(x,t)(C(x,t)-C_s(x,t))=\kappa(x,t)C(x,t)$, as shown below in the derivation of the apparent rate constant, $\kappa(x,t)$.

We now derive some relationships that will be useful in establishing and simplifying our differential equations and the associated boundary and initial conditions. In a thin bed slice of thickness Δx, the bed porosity

$$\varepsilon_b=\frac{\Omega}{A_r}=\frac{\Omega\Delta x}{A_r\Delta x}=\frac{\text{open volume}}{\text{total volume}}\ .$$

Although ε_b and Ω depend on the axial location x, we do not explicitly note that dependence here. Therefore solid volume (bed material plus biofilm growth) initially is $(A_r-\Omega(0))\Delta x$. Here we consider a single particle which consists of an inert bed granule plus its biofilm growth. Let $V(0)$ be the initial volume of the particle and let $V(t)$ be its volume at time t. The solid volume at time t is then $(A_r-\Omega(0))\Delta x\left[\frac{V(t)}{V(0)}\right]$. Let V_p be the volume of the inert bed granule and let

$\beta = \sqrt[3]{V_p/V(t)}$. If the particles are spherical, then $\beta = \frac{R_p}{R}$, where R_p is the radius of the inert core and R is the radius of the bed granule including the biofilm growth on its surface. Note that β and R both depend on x as well as t. For more general shapes, these quantities are based on the equivalent spherical radii. The ratio of the solid bed volume at time t to the total bed volume is

$$\frac{(A_r - \Omega(0))\Delta x}{A_r \Delta x} \frac{\beta_0^3}{\beta^3} = \frac{(1-\varepsilon_b(0))\beta_0^3}{\beta^3}$$

where $\beta_0 = \beta(0) = \beta(x,0)$. Thus,

$$1 - \varepsilon_b(x,t) = \Big(1 - \varepsilon_b(x,0)\Big)\left[\frac{\beta(x,0)}{\beta(x,t)}\right]^3. \tag{2}$$

As previously noted, because biofilm growth is quite slow due to limited availability of carbon sources, there are two time scales in our problem. Here we consider the fast time-scale model for biodegradation of the primary contaminant. We assume that degradation within the biofilm proceeds at the steady-state rate that would prevail for the current thickness. We employ well-developed concepts used to describe mass transfer and reactions in packed beds to derive the apparent first-order rate constant for biofilm degradation. Our derivation follows the usual effectiveness factor approach for an active catalytic layer on an inert spherical core. For details on the method, we refer the reader to [12]. The following steady-state rate balance on a single particle (i.e., inert bed material plus biofilm layer) is based on the assumption that the rate of mass transport of the contaminant to the surface of the biofilm equals its rate of reaction within the biofilm. The total reaction rate in a single particle, $r_{cp}(x,t)$, is thus given by

$$r_{cp} = \frac{4}{3}\pi(R^3 - R_p^3)E_f k_x C_s = 4\pi R^2 k_c (C - C_s), \tag{3}$$

where k_x is the first-order biodegradation rate of the substrate when the substrate molecule is in the biofilm near the active heterotroph, and $E_f(x,t)$ is the effectiveness factor. The effectiveness factor is the ratio of the actual reaction rate in the biofilm to the reaction rate that would be obtained if the concentration were C_s everywhere in the biofilm. The use of effectiveness factors is discussed fully in [12]. In particular, for this case it is shown that

$$E_f = 3\frac{\frac{coth((1-\beta)\phi)+\beta\phi}{1+\beta\phi coth((1-\beta)\phi)} - \frac{1}{\phi}}{(1-\beta^3)\phi}$$

where $\phi = R\sqrt{\frac{k_x \tau_f}{\varepsilon_p D_{AB}}}$. Here ε_p is the porosity of the biofilm, and D_{AB} is the binary diffusion coefficient for the substrate in water. Using $\beta = \frac{R_p}{R}$ in (3) and solving for C_s we obtain

$$C_s = \frac{3k_c\beta C}{R_p E_f k_x - R_p E_f k_x \beta^3 + 3k_c\beta}\ .$$

The reaction rate per bed volume, $r_{bv}(x,t)$, is given by

$$r_{bv} = \frac{1-\varepsilon_b}{4\pi R^3/3} r_{cp}\ .$$

Substituting for r_{cp}, eliminating C_s and simplifying yields

$$r_{bv} = \frac{3(1-\varepsilon_b)\beta(1-\beta^3)E_f k_x k_c C}{R_p E_f k_x - R_p E_f k_x \beta^3 + 3k_c\beta}\ .$$

Therefore, the apparent first-order rate constant, $\kappa = \frac{r_{bv}}{C}$, is

$$\kappa = \frac{3(1-\varepsilon_b)\beta(1-\beta^3)E_f k_x k_c}{R_p E_f k_x (1-\beta^3) + 3k_c\beta}.$$

Dividing by $3\beta(1-\beta^3)E_f k_x k_c$ yields the more desirable form,

$$\kappa = \frac{(1-\varepsilon_b)}{\frac{R_p}{3\beta k_c} + \frac{1}{k_x E_f (1-\beta^3)}}. \tag{4}$$

We are now ready to derive the differential equation for β. As indicated above, the rate of substrate utilization per bed volume per time is given by $\kappa C(x,t)$ where κ is the effective first-order rate constant. Let Y be the biofilm volume produced per mole of a given substrate degraded. Then $Y\kappa C(x,t)$ is the rate of biofilm produced per bed volume. Consequently, $\frac{Y\kappa C(x,t)}{1-\varepsilon_b}$ is the rate of production of biofilm volume per solid volume from growth due to metabolism of the given substrate. Suppose that f_n is the net rate of growth (or depletion, depending on its sign) of biofilm volume per biofilm volume due to other processes, e.g., deposition of microbes from the bulk flow or depletion paths such as sloughing. We then have

$$\frac{1}{V(t)}\frac{\partial}{\partial t}V(t) = \frac{Y\kappa C(x,t)}{1-\varepsilon_b} + \frac{(V(t)-V_p)f_n}{V(t)}.$$

Now

$$\frac{1}{V(t)}\frac{\partial}{\partial t}V(t) = \beta^3\frac{\partial}{\partial t}\frac{1}{\beta^3} = -\frac{3}{\beta}\frac{\partial}{\partial t}\beta.$$

The final relationship is

$$\frac{\partial}{\partial t}\beta(x,t) = -\frac{\beta(x,t)}{3(1-\varepsilon_b)}Y\kappa C(x,t) - \frac{\beta(x,t)}{3}(1-\beta(x,t)^3)f_n. \tag{5}$$

We next obtain the appropriate boundary and initial conditions. With axial dispersion included, at the entrance of the bed we use the well-established Danckwerts boundary condition,

$$A_r U C_{in} = [\Omega U_i C](0,t) - D_{ax}\left[\Omega\left(\frac{\partial}{\partial x}C\right)\right](0,t).$$

Dividing through by A_r and substituting $\Omega U_i = A_r U$ and $\varepsilon_b = \frac{\Omega}{A_r}$, gives

$$UC_{in} = UC(0,t) - D_{ax}\varepsilon_b(0,t)\left(\frac{\partial}{\partial x}C\right)(0,t).$$

At the exit the zero-gradient condition, $\left(\frac{\partial}{\partial x}C\right)(L,t) = 0$, is imposed. For initial conditions, $C(x,0)$ and $\beta(x,0)$ must be specified.

Rendering model equations dimensionless facilitates analysis by reducing the amount of computational or even experimental work needed to study a process. Using the definitions

$$\psi = \frac{C}{C_{in}}; \xi = \frac{x}{L}; \quad \text{and} \quad \tau = \frac{Ut}{L},$$

the equations can be rewritten in dimensionless form. Although any reference concentration could be used in the definition of ψ, we have used the inlet concentration, C_{in}, assumed in the present study to be constant.

The transport equation (1) in dimensionless form is

$$-\left(\frac{\partial}{\partial\xi}\psi\right)+Pe^{(-1)}\left(\frac{\partial}{\partial\xi}\left[\varepsilon_b\left(\frac{\partial}{\partial\xi}\psi\right)\right]\right)-Da\psi=\frac{\partial}{\partial\tau}[\varepsilon_b\psi,] \tag{6}$$

where $Pe=\frac{LU}{D_{ax}}$ and $Da=\frac{\kappa L}{U}$, with equation (2) used to express ε_b in terms of β. We use expression (4) to obtain the following more useful form for Da :

$$Da=(1-\varepsilon_b)\left(\frac{R_pU}{3k_cL\beta}+\frac{U}{Lk_xE_\beta}\right)^{-1}$$

where $E_\beta=E_f(1-\beta^3)$, which can then be written as

$$Da=(1-\varepsilon_b)\left(\frac{1}{3A\beta}+\frac{1}{BE_\beta}\right)^{-1},$$

or, equivalently, in a form that can be used when $E_\beta=0$,

$$Da=(1-\varepsilon_b)\left[\frac{3ABE_\beta\beta}{BE_\beta+3A\beta}\right]$$

where $A=\frac{k_cL}{R_pU}$ and $B=\frac{Lk_x}{U}$.

The dimensionless form of equation (5) is

$$\frac{\partial}{\partial\tau}\beta=\left(-\frac{\beta}{3}\right)\left[\left(\frac{3ABE_\beta\beta}{BE_\beta+3A\beta}\right)\gamma\psi+\Gamma(1-\beta^3)\right] \tag{7}$$

where $\gamma=YC_{in}$ and $\Gamma=\frac{f_nL}{U}$.

The boundary conditions become

$$\psi(0,\tau)+\left[\frac{1}{Pe}\right]\varepsilon(0,\tau)\left(\frac{\partial}{\partial\xi}\psi\right)(0,\tau)=1 \tag{8}$$

and

$$\left(\frac{\partial}{\partial\xi}\psi\right)(1,\tau)=0. \tag{9}$$

Although one compound is identified as the target pollutant, other carbon sources may be found in the groundwater. Because the growth of the biofilm is dependent on all carbon sources, it may be desirable or, in some cases, even necessary to consider two or more substrates, e.g., one being the the target contaminant and a second representing all other carbon sources. Although the extension of the above model to multiple substrates appears to be straight-forward, the correct formulation of the reaction terms for these substrates would require knowledge about the effects of the interactions on their metabolism. We note that if the respective values for the reaction rates, yield coefficients, and diffusion coefficients for all carbon sources are essentially the same, the single substrate model can be employed.

5. **Numerical methods and solution technique.** The governing equations (6) and (7) for this model are solved using an algorithm developed by Berzins and Dew implemented in the software package PDECHEB [2]. This method-of-lines approach uses Chebyshev polynomials to approximate a continuous solution of the PDEs between each pair of spatial breakpoints, giving a differential algebraic system that is subsequently solved by DASSL [3]. It is of particular significance that this software allows a coupled system of ODEs to be solved along with the PDEs. Thus the equation for β, which has the form of an ODE, is written for each spatial discretization point and is incorporated as the resulting ODE system.

6. **Determination of input parameters.** In modeling and analyzing biowall performance, ascertaining values for input parameters is an important task. It is necessary to understand the exact interpretation and use of a parameter before specifying or assigning a value to it. Values for some parameters can be obtained from experimental conditions, while others depend indirectly on measured values. In the absence of specific information, the net first-order biofilm growth or depletion rate from processes other than growth due to heterotophic metabolism, f_n, has been set to zero. We examine all other input in the order in which they are specified in the input data set. A list of the variables and the values used in our computational work are provided in Appendix B.

The bed porosity can be measured directly. It is typically in the range 0.30-0.50. The superficial velocity can be calculated directly as the flowrate divided by the total cross-sectional area. The bed length, L, is directly measurable.

The mass transfer coefficient, k_c, is obtained from a suitable correlation. Because the groundwater flows through the bed very slowly, mass transport is dominated by molecular diffusion. Mass transport to the surface of the biofilm is typically much faster than the reaction rate in the biofilm. Thus, for many practical applications, the mass transport coefficient does not have a strong effect on model predictions. Mass transfer correlations for some common low Reynolds number models can be found in [6].

The axial dispersion coefficient cannot be measured directly but can be derived from tracer experiments or estimated from established correlations. Because the Reynolds number is typically much less than one, we follow the recommendation of Wakao and Kaguei ([12], p. 87) that D_{ax} be taken to be $f \cdot D$, where D is the molecular diffusion coefficient and f is a factor in the range 0.6-0.8. We note that our computations have shown that increasing D_{ax} by a factor of 100 has no significant change in the calculated biofilm growth and target contaminant removal profiles.

The inert equivalent pellet radius, R_p, can be estimated by $\sqrt[3]{3V/4\pi}$, where V is the mean volume of an inert particle. Because modeling the initial microbial attachment of the biofilm is not in the scope of this work, we assign a small uniform initial biofilm thickness. The initial radius of the bed pellet with the biofilm, R_i, exceeds the pellet radius R_p by the initial biofilm thickness. In our computations we have used $R_p/R_i = \beta_0 = 0.9997$.

Biofilms are quite open structures, and in thin films the porosity can vary from close to 0.8 in the top layers to 0.4 in the bottom layers next to the substratum. We use a typical value of 0.75. The tortuosity factor varies as a function of porosity. A value of 1.3 is recommended. The binary diffusivity, D_{AB}, of a given substrate (such as toluene or benzene) in water can be looked up directly. Diffusivity and tortuosity factors are discussed in detail in [13].

Substrate inlet concentrations are directly measurable. The value for the first-order degradation rate of a substrate when the substrate molecule is in the biofilm, near or within the active heterotroph, k_x, should be chosen so that the effective rate realized in a given system agrees with the observed value. Its value is typically higher than published degradation rates that include mass transport and diffusional limitations. For in-situ and laboratory-determined degradation rates, we refer the reader to [9].

The volumetric yield, Y, is the volume of biomass that results from the metabolism of one mole of substrate. As an example, for benzene it is computed as follows.

Letting $Y_{DX} = 0.1$ (carbon-mole biomass/carbon-mole substrate), $m_{cm} = 0.0246$ (kg biomass/carbon-mole), $n_C = 6$ (carbon moles /mole target contaminant) and $\rho_{biofilm} = 60\ kg/m^3$, we have,

$$Y = \frac{Y_{DX} m_{cm} n_c}{\rho_{biofilm}} = 2.5 \times 10^{-4}\ m^3/mol.$$

For additional yield coefficients we refer the reader to [7].

7. **Results and discussion.** To this point we have focused on the development of our comprehensive biowall performance model, which can be used both as a design and as an optimization tool. Before we examine specific results, we explore the implications of key expressions that were derived in Section 3. Of particular importance is the local, instantaneous degradation rate, κ. As can be observed in equation (1), the term $-\kappa C(x,t)$ is the "sink" for the removal of the target contaminant. It is instructive to consider the denominator of the expression for κ given in equation (4). The first term, $\frac{R_p}{3\beta k_c}$, is the characteristic time for the transport of the substrate from the bulk flow to the surface of the biofilm. The second term, $\frac{1}{k_x E_f (1-\beta^3)}$, is the characteristic time for degradation within the biofilm. In this study, when the biofilm is initially quite thin, the mass-transport time is much less than the time for processes occurring within the biofilm (the "reaction" time). For example, using the inputs in Appendix B with β equal to 0.9997, the mass transport term is O(10^3 s), while the second term is O(10^5 s). In other words, biodegradation is initially kinetically limited.

Although we have used the full expression for κ in our calculations, it is instructive to consider the various components of the simplified expression for κ that results from omitting the mass-transport limitation, namely,

$$\kappa \approx \Big[(1-\varepsilon_b)(1-\beta^3)\Big] E_f k_x. \tag{10}$$

The factor in square brackets is the (local) fraction of bed volume that is occupied by the biofilm, i.e., the location of the active degraders. As the volume of biofilm increases, the value of β decreases. A more convenient measure of biofilm growth is $\hat{\beta} = \frac{1}{\beta}$, where $\hat{\beta}^3$ is thus the ratio of the total solids volume including the biofilm to the volume of inert bed material. As the biofilm develops, $\hat{\beta}$ increases from its initial value (approx. 1.0003 in this work). Substituting for $(1-\varepsilon_b)$ from equation (2) gives

$$\kappa \approx \Big[(1-\varepsilon_{b_0})\beta_0^3(\hat{\beta}^3 - 1)\Big] E_f k_x, \tag{11}$$

where ε_{b_0} and β_0 denote the initial values of the respective variables. From this equation, we see that this geometrical factor strictly increases as $\hat{\beta}$ increases, i.e., as the biofilm grows. It is true that as ε_b approaches zero, the bed becomes plugged and inoperable, as is reflected by the occurrence of the product $\varepsilon_b C$ in the right-hand side of equation (1). However, in this work we are far from that limit, with ε_b not dropping below 0.3.

The effectiveness factor, E_f, frequently employed in the simulation of heterogeneous catalytic processes, is a factor between zero and one that accounts for the reduction in the intrinsic degradation rate, k_x, due to time required for the substrate to diffuse into the biofilm. Although k_x is a constant, E_f depends on the thickness of the biofilm, decreasing slowly as $\hat{\beta}$ increases. Figure 2 displays the

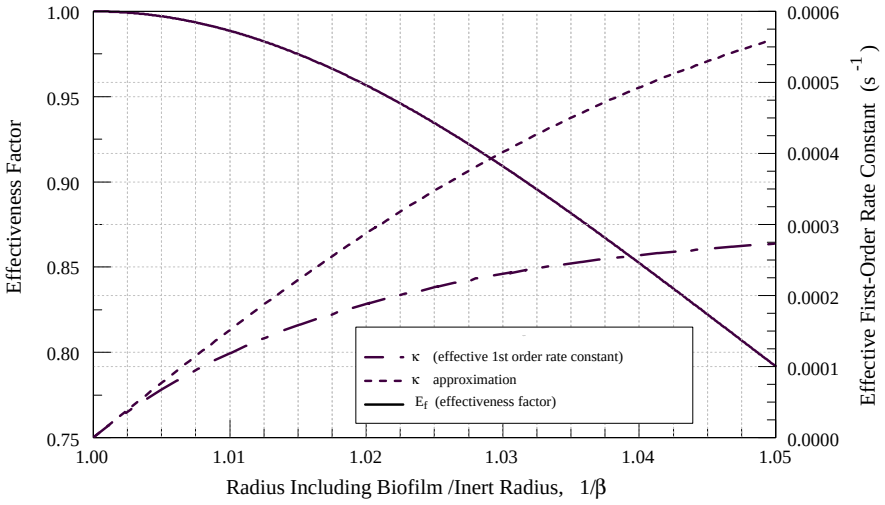

FIGURE 2. Dependence of effectiveness factor and effective first-order rate constant on biofilm thickness.

graph of E_f as a function of $\hat{\beta}$, based on our standard input values. The range of values shown for $\hat{\beta}$ corresponds to that encountered in the results that we discuss below. Over this interval, E_f decreases from unity to slightly less than 0.8, indicating the onset of a small diffusional limitation as the biofilm thickness increases by up to 5% of the effective inert pellet radius.

Also shown in Figure 2 are the exact values for κ coming from equation (4), and the approximate values from equation (10), obtained by omitting the mass-transport term. As expected, when the biofilm is quite thin, the two curves essentially coincide. As the biofilm thickness increases, the reaction rate increases and the corresponding reaction time decreases, bringing the mass-transport limitation into play. Thus, for $\hat{\beta}$ close to 1.01, although the values have diverged, the effective reaction rate is still dominated by the kinetic component. Even when the biofilm has grown to a thickness that is 5% of the inert bed particle radius, the degradation rate is controlled equally by the mass-transport and kinetic rates. Thus, throughout the range of conditions predicated in this work, actions that promote the growth of the biofilm lead to an increase in the rate of destruction of the contaminant and, consequently, to its more effective removal from the effluent stream. This observation is central to our understanding of biowall performance.

We now examine the results of exercising our model by varying certain key parameters. The availability of experimental substrate and biofilm thickness profiles as a function of time-on-stream is extremely limited. Instead of comparing specific results to particular experimental data, we examine the trends predicted using our biowall performance model in the light of the underlying biological, chemical, and physical processes involved. These trends will be shown to be consistent with the known behavior of a wide class of bioreactors. In our examples, we use the same bed length (1.52 m) and superficial velocity (7.04×10^{-6} m/s). The corresponding residence time is 2.5 days. Additional input values can be found in Appendix B.

Values listed for the substrate are representative of a contaminant that is subject to relatively slow aerobic degradation, e.g., trichloroethylene.

The effect of the development of the biofilm on target contaminant removal is displayed in Figure 3. The abscissa is the dimensionless distance into the reactor $\xi = x/L$, and the ordinate is the dimensionless concentration of the substrate $\Psi = C/C_{in}$.

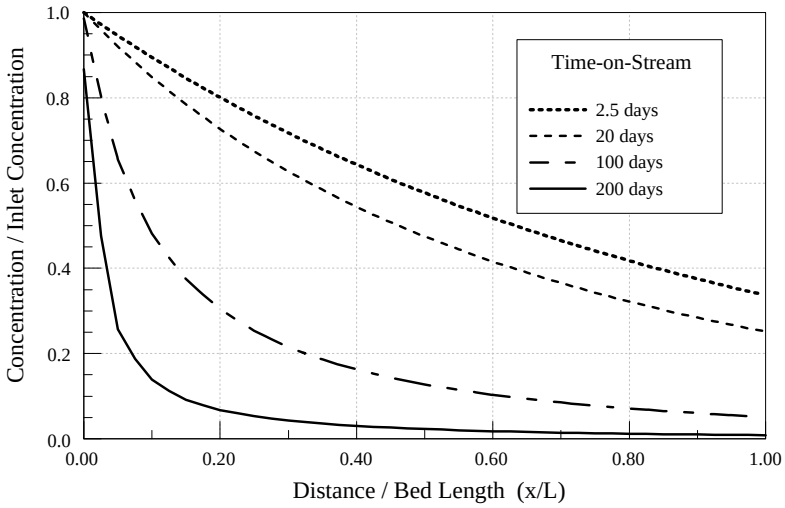

FIGURE 3. Effect of biofilm development on target contaminant profiles for various times-on-stream.

Because we have not included mechanisms for initial microbial attachment in the present model, we have assumed a uniform initial biofilm thickness throughout the bed. Even though this initial thickness is small (2 μm), it is responsible for the removal of the target pollutant for early times-on-stream, e.g., close to 2.5 days. The profile for 20 days shows a somewhat more rapid decrease in the target contaminant concentration as a function of distance into the reactor. This trend continues in the profiles obtained after 100 days and 200 days.

Here we clearly see the expected result that the growth of the biofilm leads to an increase in the degradation rate and the more effective removal of the pollutant from the effluent stream. The predicted trend of enhanced removal with increasing time-on-stream is consistent with the behavior of similar bioreactors reported in the literature (e.g., [1], [4], [5]).

For the longer times-on-stream, the profiles in Figure 3 show a much higher removal rate toward the entrance of the biowall. In fact, after 200 days on stream, 86% of the primary contaminant has been removed in the first tenth of the bed. This improved rate is due to increased biofilm thickness in that region. That is, as the substrate is degraded additional biomass is produced. Farther down the biowall the substrate concentration is lower. Therefore, less biomass is produced, and the biofilm thickness increases at a slower rate. As a result, the biofilm thickness ($\hat{\beta}$) profiles can be expected to mirror the target contaminant profiles. This phenomenon is clearly observed in Figure 4.

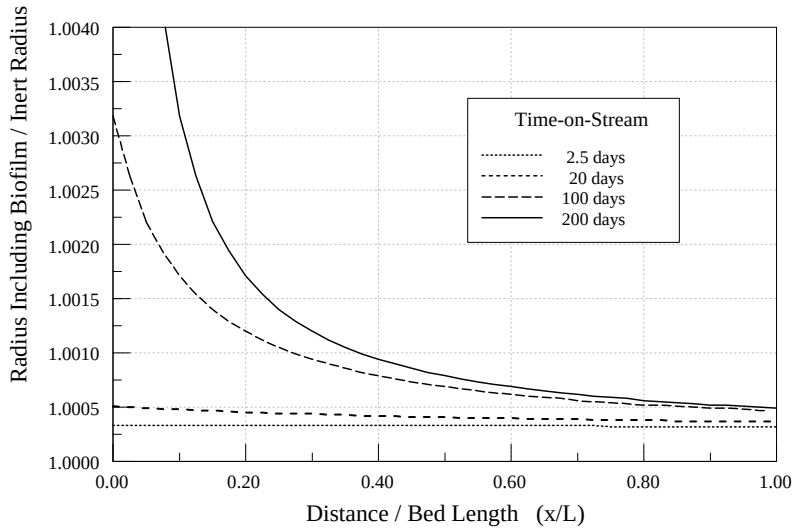

FIGURE 4. Biofilm development: Profiles of biofilm thickness for various times-on-stream.

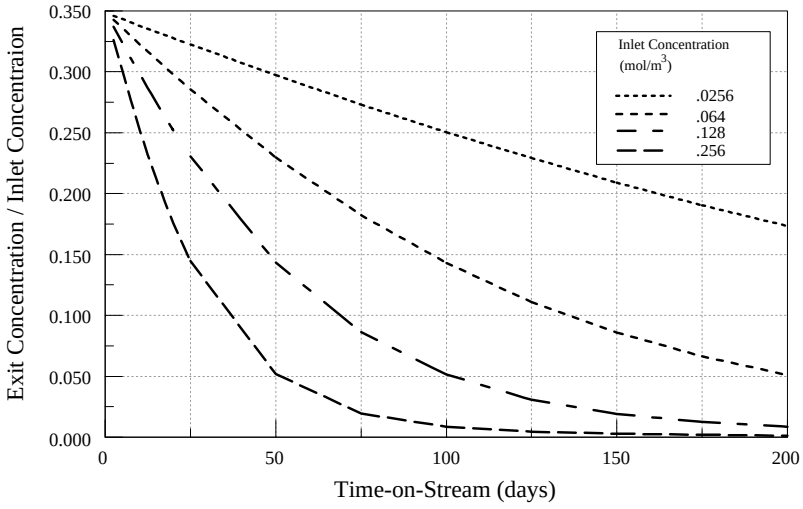

FIGURE 5. Effect of biofilm development on target contaminant removal for various inlet concentrations.

In Figure 5 the ratio of contaminant concentration at the exit of the biowall to the inlet concentration versus the time-on-stream is plotted for a range of inlet concentrations. It is evident that this dimensionless exit concentration decreases with increasing inlet concentration at any given time-on-stream. One minus this quantity gives the conversion or fraction of incoming contaminant that is degraded

in the bed. Thus the conversion increases under these conditions as the inlet concentration of the carbon source for the biofilm growth increases.

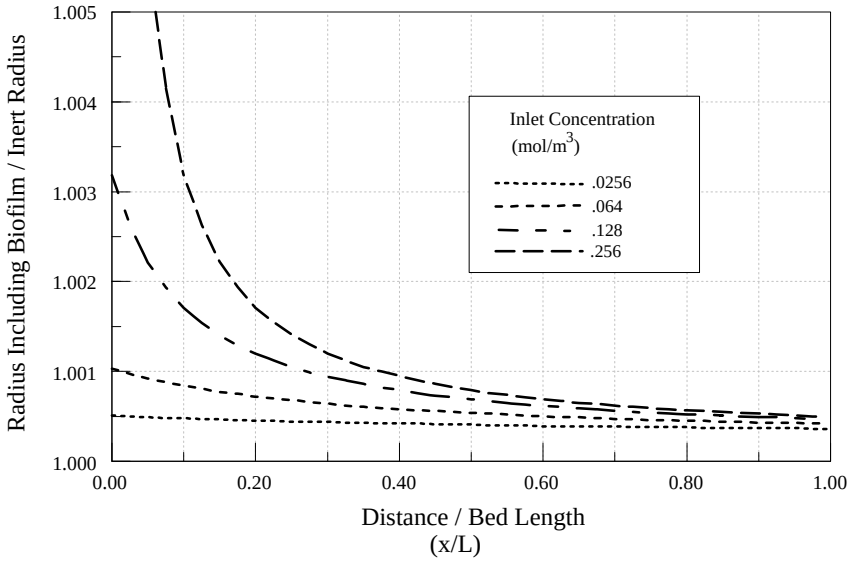

FIGURE 6. Biofilm development: Profiles of biofilm thickness at 100 days for various inlet concentrations.

Figure 6 displays the bed profiles of biofilm thickness at 100 days on stream for the same inlet concentrations. The biofilm thickness increases with higher inlet concentrations at all locations within the bed, especially towards the front. It is instructive to observe that the only way in which C_{in} enters the dimensionless equations is through the dimensionless volumetric yield, $\gamma = YC_{in}$. An increase in the inlet concentration thus gives a higher value for γ, which, as can be seen from equation (7), results in a more rapid decrease in β (increase in $\hat{\beta}$). The explanation for the improved contaminant removal is thus consistent with the previously stated principle that promoting biofilm growth leads to enhanced degradation.

We now address the sensitivity of the calculated results to key input parameters. Although there are many variables listed in Appendix A, most of them are derived from a small number of physical inputs, such as C_{in}, k_c, k_x, L, R_p, and U. As is generally the case for flow reactors, the residence time (L/U) is an important design parameter. This observation is supported by the occurrence of this ratio in all the dimensionless numbers that enter the equations with the exception of the Peclet number for axial dispersion, P_{ax}. However, as observed above, axial dispersion does not play a significant role in the flow regime in which our sample calculations have been performed. In Figure 7, we can see the effect on the exiting contaminant concentration of halving and doubling the base case residence time (2.5 days), obtained by doubling and halving the velocity, U. For these cases, the exit concentration over the range of times-on-stream plotted decreases as the superficial velocity decreases. In other words, as would be expected, the contaminant conversion increases with increasing residence time. At ten days, the conversion for

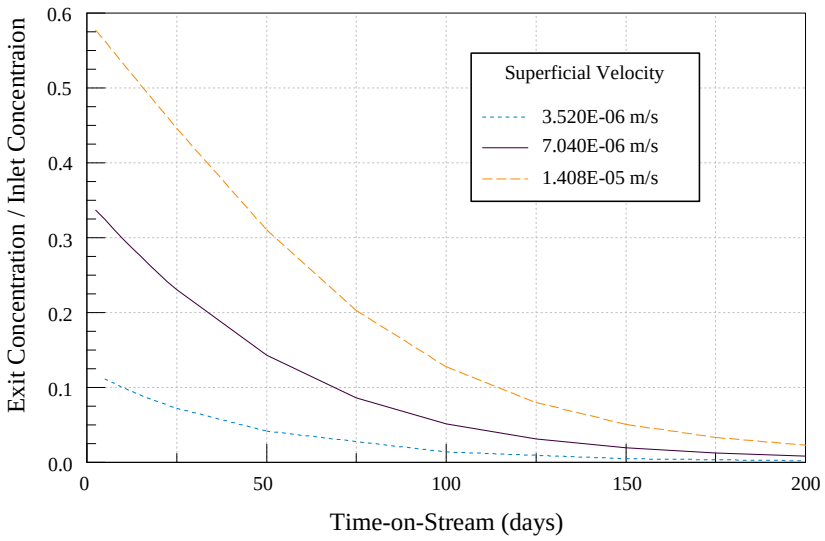

FIGURE 7. Effect of varying superficial velocity on biowall performance.

the longest residence time is approximately twice that indicated for the shortest time. However, at 100 days this ratio has decreased to approximately 1.1. The explanation for this change is that as the velocity is increased, more groundwater and thus more substrate flow through the bed. Because the growth of the biofilm is nutrient limited, its development is accelerated at higher flow rates. Consequently conversion improves over time for all cases, but it does so more rapidly at higher throughput. In the design of a biowall, it is evidently important to understand the relationship of target contaminant removal, time-on-stream, and residence time.

The transport of substrate from the bulk flow to the surface of the biofilm is incorporated in our model by the use of a mass transfer coefficient, k_c. For models based on this formulation, results can exhibit sensitivity to the value for k_c. If not experimentally determined, its value is obtained from correlations of experimental data involving dimensionless numbers that characterize the flow, in particular the Reynolds number. For the very low Reynolds number flow of this study, it is well known that there is considerable scatter in the experimental data on which published correlations depend. Consequently, there is inherent uncertainty in specifying the input value for k_c in this case. In Figure 8, exiting concentration is plotted versus time-on-stream for the base case value for k_c (1.97×10^{-6} m/s) and half and twice that value. As is readily apparent, the curves do not exhibit significant differences. This lack of sensitivity to the value used for k_c is consistent with the previous inference that for these cases contaminant removal is predominantly kinetically limited.

Because of this kinetic limitation, we would expect to find pronounced sensitivity of model predictions to the value used for the intrinsic reaction rate, k_x. That such is the case can be seen in Figure 9, in which plots of the exiting concentration versus time-on-stream for the base case value of k_x ($8.7 \times 10^{-3}\ s^{-1}$) and for half and twice

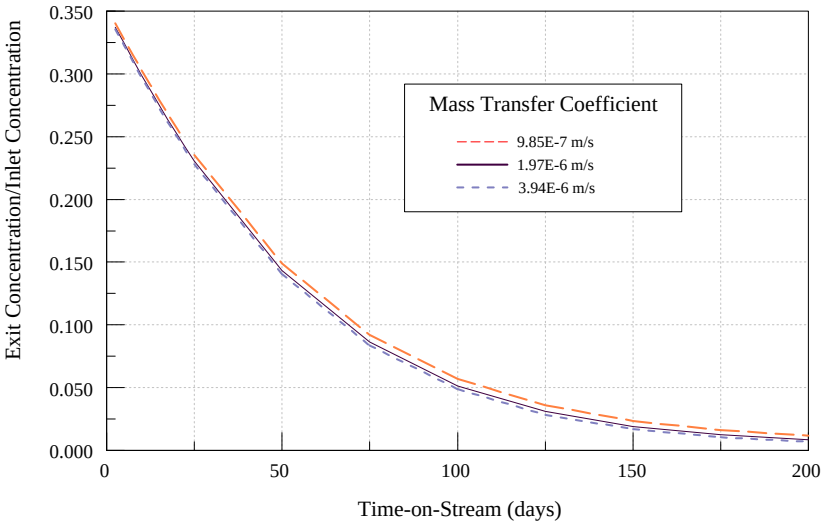

FIGURE 8. Effect of varying the mass transfer coefficient on biowall performance.

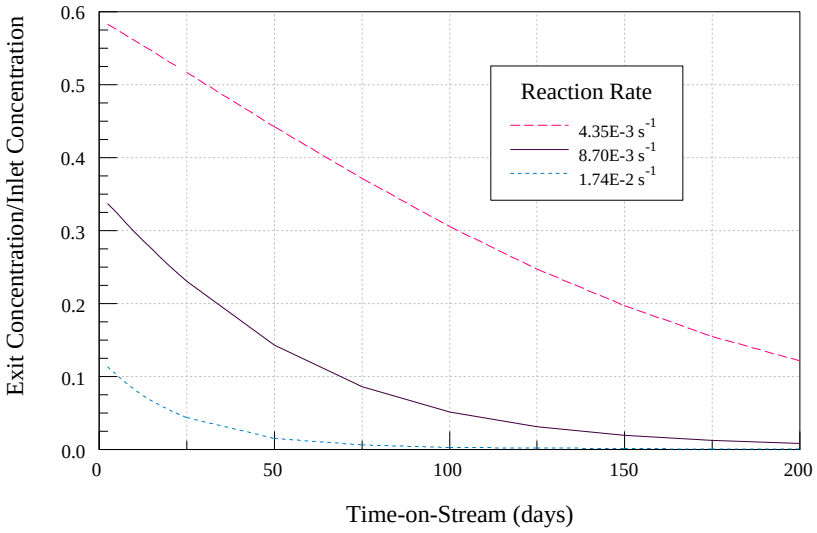

FIGURE 9. Effect of yarying the intrinsic reaction rate on biowall performance.

that rate are displayed. The sensitivity to k_x is readily apparent. At shorter times-on-stream, the ratios of the exit concentrations are of the same order as those of the corresponding reaction rates. However, for longer times-on-stream (e.g., > 50 days), the differences become much greater. This phenomenon is due to the improvement

in contaminant removal that results from biofilm development. In other words, an increase in the intrinsic reaction rate, k_x, results in greater utilization of the substrate, which in turn produces more rapid growth of the biofilm. The resulting growth of biomass gives rise to an increase in the effective rate constant, κ, and even greater substrate conversion. These observations reinforce the discussion in Section 5 concerning the need for care in determining the appropriate value for k_x for the substrate/microbe system under consideration.

8. **Summary and conclusions.** Biowall technology represents a promising approach for the remediation of many types of organic contaminants in groundwater, often at costs significantly below those of more conventional approaches. We have developed a comprehensive model for biowall performance based on accepted engineering formulations that allow consideration of the key underlying processes. Of particular significance is that the thickness of the biofilm is linked to the utilization (degradation) of the substrate. Thus the growth and distribution of the biomass within the bed and the effect of such growth on contaminant removal can be studied. Representative values for input parameters of the model were discussed and presented. The numerical solution of the governing equations has been implemented in a robust computer code.

We have explored the implications of the expression for the effective first-order degradation rate obtained in the derivation and examined both the significance and relative contributions of its components. In our examination of modeling predictions, one series of substrate and biofilm thickness profiles clearly exhibited the trend that contaminant removal is enhanced by the growth of the biofilm with increasing time-on-stream. This observation is consistent with our analysis of the effective rate constant and with experimental findings on the effect of biofilm development on performance. It is important to recall that in this work the biofilm remains sufficiently thin so that active degraders are predicated to exist down to the inert surface, with the intrinsic degradation rate limited only by diffusion within the biofilm. In another series of runs, increasing the inlet concentration of the substrate resulted in more rapid biofilm growth and consequently in enhanced conversion. This observation again agrees with the principle that the promotion of biofilm growth leads to an increase in the overall rate of biodegradation.

In examining the sensitivity of model results to key input parameters, we observed the expected dependence of initial conversion on residence time, namely, that contaminant removal increases with increasing residence time. However, when the residence time is decreased by increasing the superficial velocity, the concomitantly higher throughput of nutrient results in accelerated growth of the biofilm. Consequently, even though conversion improves over time for all cases, it does so more rapidly at higher velocity. For the operating regime that we investigated, model predictions are relatively insensitive to variation in the mass transfer rate, but exhibit a strong dependence on the intrinsic reaction rate, k_x.

In the present work, the pollutant is considered to be the sole substrate, typical of a case in which groundwater is contaminated from the release of single chemical compound. The model can, however, be easily modified to include multiple substrates with different intrinsic degradation rates and to examine the possible substrate interactions. Similarly, limits to biofilm growth, e.g., processes that lead to sloughing, have not been considered, but could easily be included given suitable formulations for such mechanisms.

9. **Appendix A: Nomenclature (SI units).**

$a(x,t)$	area for mass transfer per bed volume, (m^{-1})
A	dimensionless factor $= \dfrac{k_c L}{R_p U}, (-)$
A_r	total area of bed cross-section, (m^2)
B	dimensionless factor $= \dfrac{L k_x}{U}, (-)$
$C(x,t)$	concentration of target pollutant (substrate), (mol/m^3)
C_{in}	inlet concentration, (mol/m^3)
$C_s(x,t)$	concentration at surface of biofilm, (mol/m^3)
D_{ax}	axial dispersion coefficient, (m^2/s)
$Da(x,t)$	Damkohler number
D_{AB}	binary diffusion coefficient for substrate in water, (m^2/s)
$E_f(x,t)$	effectiveness factor, $(-)$
$E_\beta(x,t)$	modified effectiveness factor $= (1-\beta^3)E_f, (-)$
f_n	net first-order biofilm growth rate from processes other than heterotropic metabolism, (s^{-1})
k_c	mass transfer coefficient, (m/s)
k_x	first-order biodegradation rate of a substrate when the substrate molecule is in the biofilm, near or within the active heterotroph, (s^{-1})
L	bed (biowall reactor) length, (m)
Pe	Peclet number (reciprocal mass dispersion number) $= \dfrac{LU}{D_{ax}}, (-)$
$r_{bv}(x,t)$	reaction rate per bed volume, $(mol/m^3/s)$
$r_{cp}(x,t)$	total reaction rate in a single catalytic particle, (mol/s)
$R(x,t)$	equivalent radius of pellet (bed particle) including biofilm, (m)
R_p	equivalent radius of inert pellet (i.e., without biofilm), (m)
R_i	initial radius of bed pellet including biofilm, (m)
Re	Reynolds number, $(-)$
t	time, (s)
U	superficial velocity, (m/s)
$U_i(x,t)$	interstitial velocity $= \dfrac{U}{\varepsilon_b}$, (m/s)
$V(x,t)$	volume of a bed particle including biofilm, (m^3)
V_p	volume of inert bed particle, (m^3)
x	axial distance into bed, (m)
Y	volumetric yield, (m^3/mol)

Greek:

$\beta(x,t)$	biofilm growth ratio $= \dfrac{R_p}{R}$, $(-)$
γ	dimensionless volumetric yield $= YC_{in}$, $(-)$
Γ	dimensionless growth rate $= \dfrac{f_n L}{U}$, $(-)$
$\varepsilon_b(x,t)$	bed porosity , $(-)$
ε_p	porosity of biofilm, $(-)$
$\kappa(x,t)$	effective first-order rate constant, (s^{-1})
ξ	dimensionless distance into reactor $= x/L$, $(-)$
τ	dimensionless time $= \dfrac{Ut}{L}$, $(-)$
τ_f	tortuosity factor, $(-)$
$\phi(x,t)$	dimensionless factor $= R\sqrt{\dfrac{k_x \tau_f}{\varepsilon_p D_{AB}}}$, $(-)$
$\psi(x,t)$	dimensionless concentration $= \dfrac{C}{C_{in}}$, $(-)$
$\Omega(x,t)$	open area of bed cross-section, (m^2)

10. Appendix B: Biowall model input.

Bed porosity, ε_b	0.40
Superficial velocity, U	7.04×10^{-6} m/s
Bed length, L	1.52 m
Mass transfer coefficient, k_c	1.97×10^{-6} m/s
Axial dispersion coefficient, D_{ax}	2.62×10^{-7} m^2/s
Inert equivalent pellet radius, R_p	6.35×10^{-3} m
Initial pellet + biofilm radius, $R_i = R(x,0)$	6.352×10^{-3} m
Biofilm porosity, ε_p	0.75
Tortuosity factor, τ_f	1.30
Binary diffusivity, D_{AB}	1.00×10^{-9} m^2/s
Inlet concentration, C_{in}	0.128 mol/m^3
Reaction rate, k_x	8.70×10^{-3} s^{-1}
Volumetric yield, Y	2.50×10^{-4} m^3/mol

Acknowledgements. This research was partially supported by Assigned Release Time (ART) and a Center for Research (CfR) grant from William Paterson University of New Jersey.

REFERENCES

[1] Arcangeli, J. P. and Arvin, E., Growth of an Aerobic and an Anoxic Toluene-Degrading Biofilm - A Comparative Study. Water Science Technology, **8**, pp. 125–132, 1995.

[2] Berzins, M. and Dew, P. M., Algorithm 690: Chebyshev Polynomial Software for Elliptic-Parabolic Systems of PDEs. ACM Trans. Math. Software **17**(2) pp. 178-206, 1991.

[3] Brenan, K. E., Campbell, S. L., and Petzold, L. R., Numerical Solution of Initial Value Problems in Differential Algebraic Equations. North Holland, Amsterdam, 1989.

[4] Chang, Myung-Keun, Substrate Interactions During the Degradation of Benzene, Toluene, and p-Xylene and their Effects on Sorption in a Fixed-Bed BiologicalActivated Carbon Reactor. UMI Dissertation Services, 1994.

[5] Freitas dos Santos, L. M. and Livingston, A. G., Membrane-Attached Biofilms for VOC Wastewater Treatment II: Effect of Biofilm Thickness on Performance. Biotechnology and Bioengineering, **47**, pp. 90-95, 1995.

[6] Geankopolis, C. J., Transport Processes and Unit Operations., 3^{rd} edition, Prentice-Hall, Englewood Cliffs, N.J., p. 448, 1993.

[7] Heijnen, J. J. and J. P. Van Dijken, In Search of a Thermodynamic Description of Biomass Yields for the Chemotrophic Growth of Microorganisms. Biotechnology and Bioengineering, **19**, pp. 833–858, 1992.

[8] Horn, H. and Hempel, D. C., Substrate Utilization and Mass Transfer in an Autotrophic Biofilm System: Experimental Results and Numerical Simulation. Biotechnology and Bioengineering, **53**, pp. 363–371, 1997.

[9] Nielsen, P. H., Bjerg, P. L., Smith, P., and Christensen, T. H., In Situ and Laboratory Determined First-Order Degradation Rate Constants of Specific Organic Compounds in an Aerobic Aquifer. Environmental Science and Technology, **30**, pp. 31–37, 1996.

[10] Reichert, P., AQUASIM 2.0 User Manual, Computer Program for the Identification and Simulation of Aquatic Systems, Swiss Federal Institute for Environmental Science and Technology, Dbendorf, Switzerland, 1998.

[11] Sharp, R. and Landowski, G., Factors Affecting Ultra Microbacteria Biobarrier Design: Nutrient/Bacteria Delivery, Biomass Distribuation and Formation, and Hydrodynamic Effects. Hazardous Substance Management Research Center, NSF Industry/University Cooperative Center of the New Jersey Commission of Science and Technology, Final Report Site 49, March 1999.

[12] Wakao, N. and Kaguei S., Heat and Mass Transfer in Packed Beds. Gordon and Breach, New York, 1982.

[13] Zhang, T. C. and Bishop, P. L., Evaluation of Tortuosity Factors and Effective Diffusivities in Biofilms. Water Resources, **28**(11), pp. 2279-2287, 1994.

Received on March 31, 2005. Accepted on March 15, 2006.

E-mail address: fengyad@wpunj.edu
E-mail address: stevensj@mail.montclair.edu